An Adaptively Parameterized Algorithm Estimating Respiratory Rate from a Passive Wearable RFID Smart Garment

Robert Ross Drexel University College of Engineering Philadelphia, PA USA 0000-0002-0726-4741 William M. Mongan Drexel University College of Engineering Philadelphia, PA USA 0000-0002-4122-5156 Patrick O'Neill

Drexel University

College of Computing and Informatics

Philadelphia, PA USA

po73@dragons.drexel.edu

Ilhaan Rasheed
Drexel University
College of Engineering
Philadelphia, PA USA
ilhaanrasheed@gmail.com

Adam Fontecchio Drexel University College of Engineering Philadelphia, PA USA af63@drexel.edu Genevieve Dion

Drexel University

College of Media Arts and Design

Philadelphia, PA USA

gd63@drexel.edu

Kapil R. Dandekar Drexel University College of Engineering Philadelphia, PA USA 0000-0003-1936-2514

Abstract-Currently, wired respiratory rate sensors tether patients to a location and can potentially obscure their body from medical staff. In addition, current wired respiratory rate sensors are either inaccurate or invasive. Spurred by these deficiencies, we have developed the Bellyband, a less invasive smart garment sensor, which uses wireless, passive Radio Frequency Identification (RFID) to detect bio-signals. Though the Bellyband solves many physical problems, it creates a signal processing challenge, due to its noisy, quantized signal. Here, we present an algorithm by which to estimate respiratory rate from the Bellyband. The algorithm uses an adaptively parameterized Savitzky-Golay (SG) filter to smooth the signal. The adaptive parameterization enables the algorithm to be effective on a wide range of respiratory frequencies, even when the frequencies change sharply. Further, the algorithm is three times faster and three times more accurate than the current Bellyband respiratory rate detection algorithm and is able to run in real time. Using an off-the-shelf respiratory monitor and metronome-synchronized breathing, we gathered 25 sets of data and tested the algorithm against these trials. The algorithm's respiratory rate estimates diverged from ground truth by an average Root Mean Square Error (RMSE) of 4.1 breaths per minute (BPM) over all 25 trials. Further, preliminary results suggest that the algorithm could be made as or more accurate than widely used algorithms that detect the respiratory rate of non-ventilated patients using data from an Electrocardiogram (ECG) or Impedance Plethysmography (IP).

Index Terms—biomedical signal processing, parameter estimation, wearable sensors, filtering algorithms

I. INTRODUCTION

Currently, many respiratory monitoring systems utilize sensors attached to a patient's body. These sensors are then connected by wires to machines which process, record, and display the patient's respiratory information. Al-Khalidi, *et al* provide an overview of respiration monitoring systems, and

concludes that most respiration monitoring systems involve wired sensors directly attached to patients [1].

Wired sensors have several negative effects: staff and patients can pull the wires, causing detachment and/or pain; wires can obscure the patient's body, inhibiting evaluations and procedures, and they tether the patient to a location; the most accurate wired sensors require a mask or intubation, causing discomfort, distress, and distortion of the respiratory pattern. Respiratory monitoring is a standard component of care in Neonatal Intensive Care Units (NICU), but premature babies have a limited surface area and adhesive sensors may not be desirable on their developing skin [2], [3].

Of even greater concern, the wired systems most commonly used on non-ventilated patients are surprisingly inaccurate. Charlton et al [4] tested several hundred algorithms which estimated respiratory rate from two of the most common signals: Electrocardiogram (ECG) and Photoplethysmogram (PPG), and compared algorithm performance to algorithms using another common signal, Impedance Plethysmography (IP), "the clinical standard for continuous respiratory rate measurement in spontaneously breathing patients." Of the hundreds of algorithms that they tested, the best algorithm had a bias of 0 breaths per minute (BPM) and a 95% Limits of Agreement (LOA) of -4.7 to 4.7 BPM. Thus, the best algorithm available for estimating respiratory rate from ECG, PPG, or IP gives results within 4.7 BPM of the true rate only 95% of the time. Therefore, there is a need, not only for a wireless respiratory rate monitor, but also a more accurate one.

The Bellyband project aims to improve over other biometric monitoring systems with a wireless, passive RFID, smartfabric sensor (the Bellyband). The Bellyband project is a collaboration among computer scientists, electrical engineers, materials scientists, fashion designers, sociologists, and med-



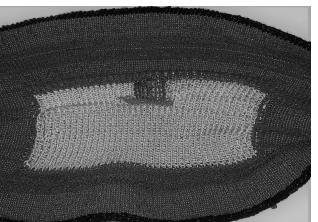


Fig. 1: Left: the Bellyband on an animatronic mannequin called a SimBaby [5]. Right: close up of the antenna portion of the Bellyband. Note the darker non-conductive material, the lighter conductive thread antenna, and the grey square inlaid in the lighter thread, which is a non-conductive pouch housing an RFID chip and matching circuit.

ical doctors [6]–[9]. The band (see Figure 1) is a cylindrical, knit band, about 8 cm wide, and long enough to stretch entirely around the abdomen of a patient. Most of the band is made of flexible, non-conductive thread. A small section (5 cm by 12 cm) is made of a flexible, stretchable, conductive, silvercoated nylon thread. The conductive thread is knit in such a way as to create an antenna. An RFID chip is inserted into a pouch on the band, and connected to the antenna [7].

The Bellyband can be used to measure several biological processes in patients, such as respiration and uterine contraction. As the wearer breathes, experiences a uterine contraction, *etc.*, the garment stretches and deforms its the knitted antenna, yielding changes in Received Signal Strength Indicator (RSSI) power [10] without requiring a transducer or other tethered sensor. It uses a Magicstrap RFID LMXS31ACNA-011 chip [11] or Monza X Dura chip [12]. The chip is interrogated by an Impinj R420 interrogator [13] using a RFMAX S9028PCLJ antenna [14]. The RFID interrogator operates within the 902-928 MHz unlicensed frequency band in the United States, and the knitted antenna and tag are impedance matched to 870 MHz [7] to facilitate oscillatory strengthening and weakening of the observed RSSI as the wearer stretches and relaxes the band during respiratory activity.

When interrogated within range, the Bellyband tag emits a signal containing its identifier, which is then received by the interrogator. Each time the return signal is received by the interrogator, the interrogator logs the return signal's arrival time, and strength, phase, and Doppler shift relative to the original interrogation wave. We use a combination of these features (e.g. RSSI, Doppler shift, and relative time stamp) to draw conclusions about various medical states of the patient wearing the Bellyband. Previously, the Bellyband has been used to detect respiratory rate [15] as well as apnea. In section V, the method proposed in this paper is compared to the GMM-based fusion algorithmdeveloped in [15], demonstrating significant improvement in detection and in runtime performance.

A system level block diagram is described in Figure 2. As shown in the figure, the smart fabric Bellyband is interrogated by an RFID interrogator, and the physical properties of the resulting backscatter are affected by changes in the Bellyband

structure. In particular, the antenna stretches and relaxes as the wearer breathes, tuning and de-tuning the antenna and changing the corresponding RSSI and phase shift. These physical properties are stored and processed as time-series data sets in or near enough to real-time to provide meaningful biomedical estimates about the wearer's state, *i.e.*, respiratory rate (RR).

A. Bellyband Relative Signal Strength Model

The Received Signal Strength Indicator (RSSI) is a function of distance between the interrogating antenna and the Bellyband d, Bellyband antenna gain G, and radar cross section of the Bellyband's antenna σ , all three of which are, in turn, functions of respiration. On inhalation, the distance between the interrogator and the tag decreases, increasing RSSI by a factor of d^4 . In addition, the Bellyband antenna's gain increases, increasing RSSI by a factor of G^2 . Finally, the radar cross section of the tag's antenna increases, increasing RSSI linearly as shown in Equation 1 [16]:

$$RSSI = \frac{P_r}{P_t} = Round \left(\frac{G^2 \lambda^2 \sigma}{(4\pi)^3 d^4} + \nu \right)$$
 (1)

Where:

RSSI = The Received Signal Strength Indicator

 $\frac{P_r}{P_t}$ = the ratio of power received to power transmitted G = the interrogating antenna's gain, a function of respiration

 λ = the interrogation wavelength. $\frac{\text{speed of light}}{\text{interrogation frequency}}$

 σ = the radar cross section of the tag's antenna, a function of respiration

d= the distance between the interrogator and the tag, a function of respiration

 ν = the noise due to multipath and other indeterminate factors.

Thus, subject respiration results in a quantized, fluctuating wave in the RSSI *vs* time graph. See the top graphs of Figures 3 and 6 for a visualization of this quantized fluctuation.

B. Motivation for the Respiratory Rate Detection Algorithm

The Bellyband's use of passive RFID offers several benefits for bio-signal detection. Tags do not require batteries or wires, resulting in a small form factor, suitable for wearable garment integration. Tags transmit a configurable unique identifier, devoid of personally identifiable information over the air. Thus, the Bellyband is comfortable, easy to put on and take off, contains no wires or batteries, and uniquely identifies patients in a HIPAA-compliant way.

However, using RFID for respiratory monitoring presents challenges: its signal decays quickly as the interrogation distance is increased, the reflected RFID signal is affected by multipath fading which result in perturbations unrelated to patient respiration, and some interrogators discretize the RSSI measurement which introduces sensor noise.

In this paper, we present an algorithm which responds to these challenges. The algorithm first smooths the noisy, discretized signal with a Savitzky-Golay filter, then counts

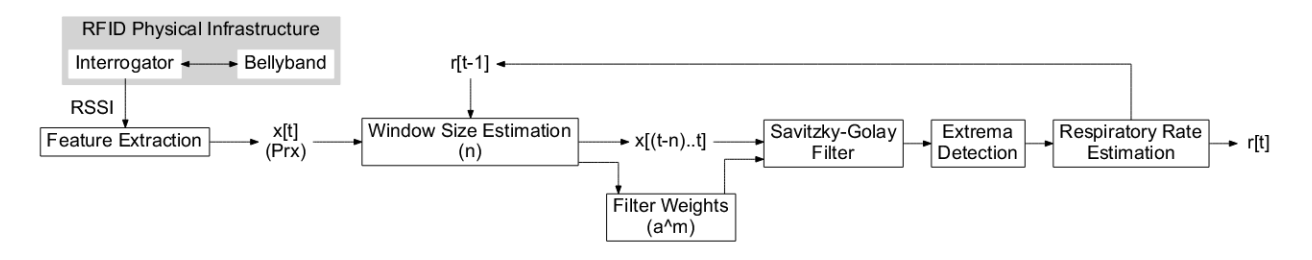


Fig. 2: A system level block diagram from which our adaptive filtering parameterization algorithm will operate, resulting in a smoothing of RFID input signals and an algorithm to dynamically estimate the user's respiration rate.

the peaks in the smoothed signal. The Savitzky-Golay filter is adaptive, in that it uses the number of respirations which were detected in the previous time window to set the number of points which are fitted to a 3rd degree polynomial in the current time window. The algorithm is fast enough to run in real time, and smooths the signal effectively even when respiratory rate varies drastically. The algorithm is general enough to be used to monitor a variety of signals whose frequency varies over time. We demonstrate the effectiveness of the algorithm on real world respiratory data.

C. Paper Outline

The rest of this paper will proceed as follows: In Section II, we summarize the state of the art in wireless respiratory rate detection and outline past work using Savitzky-Golay filters. In Section III, we describe the algorithm itself. In Section IV, we describe the data gathering and algorithm testing methodology. In Section V, we describe and discuss the results of the testing, comparing the current algorithm with the previous state-of-the-art, and in Section VI we conclude and point to future work.

II. RELATED WORK

A. Respiratory Rate Monitors

There are many systems which attempt to measure respiration rate wirelessly. Several use Wi-fi, such as Vital Radio [17], TR-Breath [18], and others [19]. These approaches measure the respiratory rate of each person within a certain radius, and are unable to uniquely identify the person to whom the respiratory rate belongs, which is important in a hospital setting. Our system uniquely identifies each Bellyband signal based on the band's tag ID. Other approaches use optical systems to measure respiratory rate [20] [21]. These approaches tether a patient to a location, just as a wired sensor would. Our system can be configured to allow greater patient mobility without loss of signal. There are also commercially available respiratory rate monitors [22]. However, their accuracy is insufficient for sick patients in a hospital [23]. Our system aims to provide higher accuracy.

B. Adaptive Savitzky-Golay Filters

The Savitzky-Golay Filter was introduced in 1964 as a way of smoothing noisy data without significantly inhibiting the underlying signal [24]. For a more detailed explanation of Savitzky-Golay filters, see Schafer's piece [25]. Others have demonstrated the effectiveness of a Savitzky-Golay filter that adapts the number of points used (n) [26] and demonstrated the benefits of applying such a filter to an Electroencephalogram (EEG) signal [27]. This paper attempts to further this previous work in two important ways. First, previous work pointed to the existence of an optimal parameterization of the Savitsky-Golay filter, however, did not provide a method for discerning that optimal parameterization other than exhaustive search over a parameter search space. Our algorithm provides a method for determining and using a sufficiently good parameterization that is fast enough for use in real time applications. Second, previous work demonstrated an adaptively-parameterized Savitzky-Golay filter's effectiveness on synthetic data. We demonstrate the effectiveness of the current algorithm using real-world data, using a second, wired sensor to provide ground truth.

III. ALGORITHM AND MATHEMATICAL MODEL

The algorithm begins by observing a window of W seconds of time-stamped RSSI values (values are in units of dBm) from the Bellyband. The window begins W seconds before the present moment and ends at the present moment.

The RSSI dynamic range is typically 3 to 4 dBm in our applications, and the signal is quantized and noisy. Therefore, first, the RSSI values of the signal are smoothed and denoised with an adaptive Savitzky-Golay filter [24]. Next, the window of filtered RSSI values is scanned for relative extrema: peaks or valleys in the time-ordered RSSI data that differ from the immediately previous relative extremum by a certain amount (Δ_y) . These relative extrema are placed in a list, and the times of the first and last relative extrema (t_i) and t_f) are noted.

The window's average respiratory rate, which is output as the present moment's instantaneous respiratory rate, is calculated per Equation 2:

$$r = \frac{\frac{1}{2}(z-1)}{t_f - t_i} \times 60 \tag{2}$$

Where:

z = the number of extrema in the window

 t_f = either the time (in seconds) of the final extremum or the time (in seconds) of the final point in the window, as observed by that point's time of arrival

 t_i = either the time (in seconds) of the initial extremum or the time (in seconds) of the initial point in the window, as observed by that point's time of arrival

This respiratory rate is used to parameterize the Savitzky-Golay filter on the next Δ_w sliding time window.

One of the key features of the algorithm is its application of an adaptive Savitzky-Golay filter. The filter fits a k^{th} order polynomial to a set of n sequential points in the data. k and n are both parameters to the filter. Because the data points are equally spaced (in time), for any given k, the n-length vector of weights for the Savitzky-Golay filter is known and only needs to be computed one time. (The weights are calculated to minimize the least squares difference between a polynomial of degree k and the data points.) Thus, the filter can be used with negligible speed cost.

The challenge for every application which uses the Savitzky-Golay filter is to choose the parameters n and k to best preserve the signal while reducing the noise. All other things being equal, we preferred a smaller k value as this simplifies the model and makes the model more robust to noise in the signal. We also wanted the filter to model an entire respiratory cycle (requiring a k of at least 3) to decrease the noise associated with respiratory rate changes within a single respiratory cycle. Thus, we chose k=3 because three is the smallest value of k able to model a single respiratory cycle, with both a peak and a trough.

The more significant challenge when detecting respiratory rate is that the period of the RSSI wave varies with the underlying respiratory rate. Thus, the parameter n must be adapted.

A well-adapted Savitzky-Golay filter might fit a 3^{rd} order polynomial to the data from half a period of the oscillating RSSI wave. The number of points in that half a period, which will be passed to the filter as parameter n, can be calculated as follows in Equation 3:

$$n = \left\lceil \frac{1}{2} \times \frac{s \times 60 \frac{\text{sec}}{\text{min}}}{r} \right\rceil \tag{3}$$

Where:

n =the number of points in half a period of the RSSI wave

s =the sample rate in Hz

r =the actual respiratory rate in BPM

For example, suppose that an respiratory rate of 70 BPM is sampled at 25 Hz. Then, using equation 3, each half breath would take place over 11 points (n=11). Suppose instead that the underlying respiratory rate is 15 BPM. Now, each half breath would take place over 50 points. Savitzy-Golay filters require n to be odd, so we set n=51.

A. Dynamic Savitzky-Golay Filter

The Savitzky-Golay filter was chosen for this algorithm because the underlying oscillatory human respiratory pattern: 'inhale, pause, exhale, pause, repeat' can be well fitted by a

low-degree polynomial even when the period of the respiratory curve is not constant (as shown in Figure 6c). In addition, the underlying noise is indeterminate and is best modeled as a normal distribution.

However, dynamic processes such as respiratory behavior are not well modeled by filtering algorithms using a fixed parameterization strategy. In Figure 3, observe that a 3rd order polynomial fitted to 11 points is well adapted to 70 BPM data but is poorly adapted to 15 BPM data, and a 3rd order polynomial fitted to 51 points is well adapted to 15 BPM data but is poorly adapted to 70 BPM data. We seek a filter that is well adapted to both 15 BPM and 70 BPM data (and to data reflecting even more extreme respiratory rates), and achieve this through an efficient, dynamic, and adaptive parameterization of the Savitzky-Golay filter.

The problem is solved by setting parameter n for the current window according to the estimated respiratory rate of the previous window, creating an adaptive Savitzky-Golay filter. Allowing the filter to adapt its value of n based on the estimated respiratory rate of the previous window fits our intuition about human respiration: respiratory rate rarely jumps significantly and instantaneously. In addition, the algorithm contains an additional feature which makes it robust against the rare case of an extreme and instantaneous respiratory rate change. We describe this feature in section III-B.

1) Selecting the Multipass Filtration Order: The dynamically parameterized Savitzky-Golay filter, like a traditional Savitzky-Golay filter, smooths the datastream by fitting the points in the datastream to a polynomial of a certain order and width [28]. Unlike a traditional Savitzky-Golay filter, the dynamic filter chooses the particular width it will seek based on the respiratory rate it has perceived most recently. In this way, the dynamic filter smooths non-dominant frequencies while leaving the dominant frequency largely unaffected.

The Savitzky-Golay filter is a convolution, and so applying it to the datastream corresponds to multiplication of the datastream's frequency domain transform. Further, repeated application of the filter has a multiplicative effect. Thus, repeated application of the filter results in additional smoothing of non-dominant frequencies [29]. Figure 4 graphs the result of four successive applications of the same filter to two different datastreams: one reflecting low-frequency respiration and one reflecting high-frequency respiration. We observe the most significant improvement to signal clarity in the first or second filtration in all trials, followed by improvements of diminishing significance upon each successive filtration. Thus, we empirically-define an optimal number of filtrations (denoted by m), which takes into account signal clarity and dynamic range achieved from repeated filtrations. Others have also demonstrated the value of this process [30]. For each of the m filtrations, the same filter parameters (i.e., polynomial order k and number of points n) are used for each filter pass. Table I records the effect of the same four successive filtrations on the dynamic range of the two particular datasets. The table shows that, even with four filtrations, the primary signal decays less than 10%.

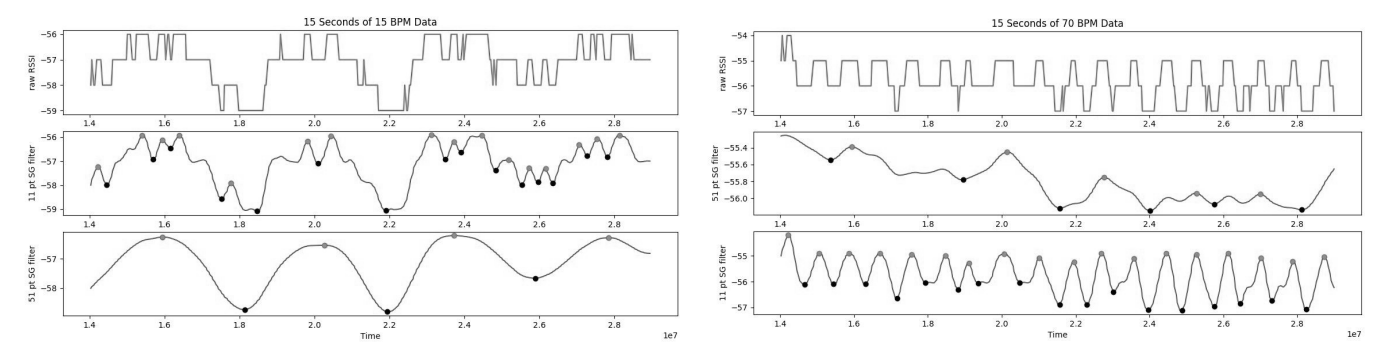


Fig. 3: Two sets of data filtered by two Savitzky-Golay Filters (the left image is RSSI for 15 BPM of respiration vs Time in μs), and the right image is RSSI for 70 BPM of respiration vs Time in μs). In each image, the top graph shows the raw RSSI data. The middle graph shows the same data filtered with an incorrectly parameterized Savitzky-Golay filter (n=11). The bottom graph shows the same data filtered with a correctly parameterized Savitzky-Golay filter (n=51). In the middle and bottom graphs, the black and grey dots show the extrema detected by the algorithm after filtering. Note that each filter is well adapted to one of the datasets, and that neither filter is well adapted to both datasets. Note also that the dynamic range of the 70 BPM data is smaller than that of the 15 BPM data, as the subject's abdomen was unable to displace as far when breathing at 70 BPM compared to 15 BPM.

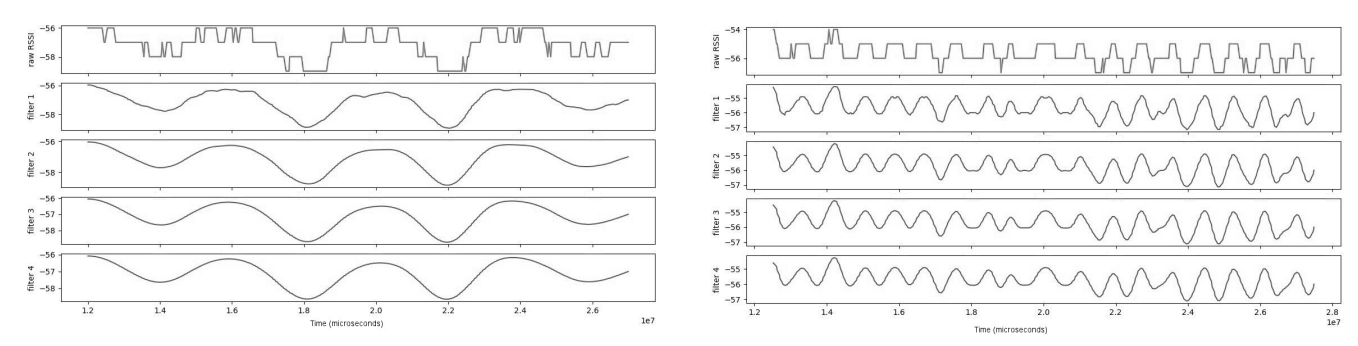


Fig. 4: Two sets of data: the left figure is RSSI for low-frequency (15 BPM) respiration, and the right figure is RSSI for high-frequency (70 BPM) respiration, vs time in μs . Each image shows five graphs, each showing an additional filtration of the RSSI. Note that, for both datasets, after the second filtering, additional smoothing is insignificant.

TABLE I: Dynamic range of the signal from two different datasets, one reflecting a 15 BPM respiratory rate and one reflecting a 70 BPM respiratory rate. Note that the overall decrease in dynamic range is less than 10%.

Filtration Level	15 BPM	70 BPM
Raw signal	3.000	3.000
Filter 1	2.999	2.949
Filter 2	2.788	2.925
Filter 3	2.678	2.878
Filter 4	2.583	2.845

Regardless of the value of m, the application of m filtrations will not entirely eliminate non-dominant-frequency, low-magnitude modulations from the data. Thus, when relative extrema are counted in the filtered signal, relative extrema with an amplitude smaller than a certain threshold (denoted by Δ_y) are excluded from the total count. Δ_y is based upon the dynamic range of the overall window of the filtered signal.

Due to the distributed property of convolutions, the multipass filter can be prepared a priori by convolving the coefficients (or multiplying the corresponding frequency spectra) with themselves until the desired order is obtained. Thus, the computational complexity of constructing an m^{th} order Savitzky-Golay filter (which filters m times) amounts to the offline-computable exponentiation of the Savitzky-Golay weight vector ${\bf a}$. By computing ${\bf a}^m$, we obtain an Savitzky-Golay weight vector that achieves the desired convolutional effect in the time domain without the need to iteratively convolve the signal. This equivalence is shown in Equation 4 [31], where ${\cal F}$ denotes the Fourier Transform.

$$a * x = \mathcal{F}^{-1}(\mathcal{F}(a)\mathcal{F}(x))$$

$$a * (a * x) = \mathcal{F}^{-1}(\mathcal{F}(a)\mathcal{F}^{-1}(\mathcal{F}(a)\mathcal{F}(x)))$$

$$a * (a * x) = (a * a) * x = \mathcal{F}^{-1}(\mathcal{F}(a)^2\mathcal{F}(x))$$

$$(4)$$

The Savitzky-Golay filter smooths data in the time domain,

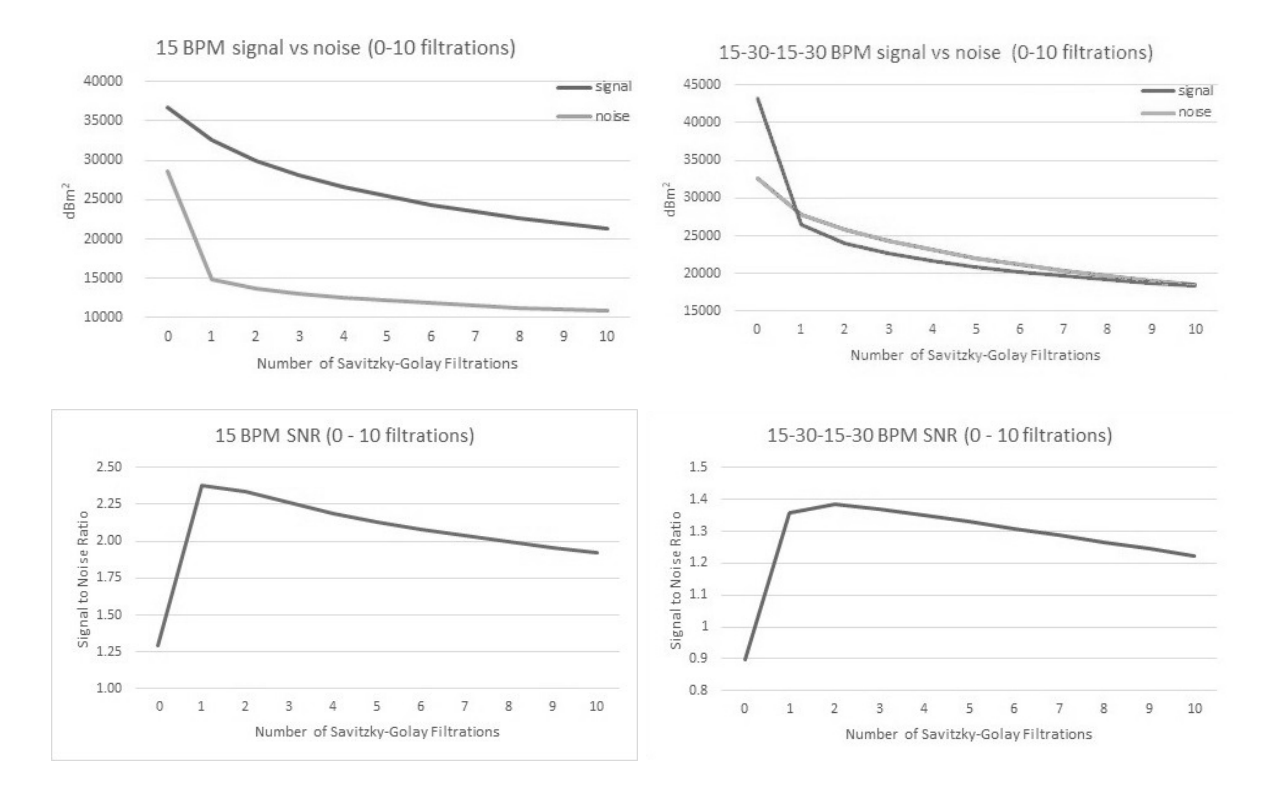


Fig. 5: Effect of running Savitzky-Golay filter 0 to 10 times on two datastreams. (The filter can be run an arbitrary number of times.) Top Graphs: Signal strength and noise strength (y-axis) vs number of filtrations (x-axis) on a dataset where the subject breathed at a constant 15 BPM (left) and where the subject's respiratory rate alternated between 15 and 30 BPM (right). Bottom Graphs: Signal-to-Noise ratio of the same two datasets (y-axis) vs the number of filtrations (x-axis): a constant 15 BPM (left) and 15, 30 BPM alternation (right). Note that for the 15 BPM dataset, maximum SNR occurred at 1 filtration, while at the 15/30 BPM dataset, maximum SNR occurred at 2 filtrations.

but has limited attenuation of higher frequencies regardless of polynomial order [28]. To improve upon the low-pass filtration of the Savitzky-Golay frequency response, a multipass approach is employed [29] in which the filter is applied multiple times in an iterative manner. Because the convolution of the Savitzky-Golay filter window with the input data corresponds to multiplication in the frequency domain, repeated application of the filter has a multiplicative effect on the frequency response on the same order as the number of passes selected. The multiplicative effect attenuates non-dominant frequencies relative to the dominant one, and sacrifices signal dynamic range for enhanced low-pass filtering. The high frequency artifacts present in the 15 BPM plot of Figure 3 are attenuated by the application of a second filter pass, while the dominant high-frequency observed in the 70 BPM plot of Figure 3 is generally unaffected in the frequency domain. The same filter parameters (i.e., polynomial order and window size) are used for each filter pass, so that at least one-half respiratory period is present in the window during filtering, facilitating attenuation of relatively high-frequency artifacts that are generally periodic within that window as discussed in Section III-A.

The benefit of attenuation diminishes as the number of passes increases, as the dynamic range of the signal is reduced; it is infeasible to eliminate artifact components entirely without sacrificing useful signal. Therefore, a limited number of filter passes is taken (denoted by m), even though this will leave behind a high-frequency, low magnitude modulation within the data. When the difference of the filtered time-series is taken for purpose of identifying respiratory peaks, modulated peaks with amplitude smaller than a dynamic threshold (denoted by Δ_y) based upon the dynamic range of the overall window are discarded following the low-pass filter. By the distributed property of convolutions, the multi-pass filter can be prepared a priori by convolving the coefficients (or multiplying the corresponding frequency spectra) with themselves until the desired order is obtained.

B. Filtering High Variation Data

As long as k < n-1, n and k are both positive integers, and n is odd, the Savitzky-Golay filter will find a unique, best fitting of a k^{th} degree polynomial to n points. This robustness is an important strength, but is accompanied by a less obvious weakness. As long as the above parameter limitations are met, a k^{th} degree polynomial will always fit n-1 points 'better'

(defined as returning a lower sum of the squared difference) than it fits n points.

Thus, there is no way to compare the fit of two filters with different n parameters or to verify that a particularly parameterized polynomial does not overfit or underfit the data. As shown in Figure 3, an incorrectly parameterized filter will not return an error - it will simply fit the best k^{th} degree polynomial to the n points it can. Thus, the question arises, 'how can we ensure that the filter is not grossly underfitting (or overfitting) the data, resulting in the algorithm underestimating (or overestimating) the respiratory rate?'

In initial testing, our filter proved robust against instantaneous decreases in respiratory rate from 175 BPM to 15 BPM, with its estimate converging to 15 BPM within 2 seconds. However, the filter was not robust against instantaneous increases in respiratory rate of more than 40 BPM. When faced with increases in respiratory rate of this magnitude, the filter would consistently underfit the post-increase data and diverge towards a 0 BPM estimated rate until the actual respiratory rate dropped back to within 40 BPM of its estimate.

Thus, an additional step in the filtration portion of the algorithm was added to protect against divergent underfitting. At the end of the respiratory rate calculation for each window, if the estimated respiratory rate for the window drops below a threshold of the lowest feasible respiratory rate r_{ll} , we classify an apnea condition [32].

If there is no apnea, the algorithm resets the filter's number of points parameter (n) as if the estimated respiratory rate from the previous window was sufficiently high (r_{reset}) , and runs again on the current window. The algorithm stores the respiratory rate calculated during this $2^{\rm nd}$ run as the estimated respiratory rate for the window, and progresses to the next window. With this addition, the filter is able to converge to any biologically feasible respiratory rate.

Our datasets contained moderate and extreme instantaneous jumps in respiratory rate. Figures 6c and 6d show that the adaptive filter handled these transitions well. Table III, row 6, shows the results of running the algorithm on datasets that contained extreme and instantaneous respiratory rate jumps from 10 BPM to 70 BPM. On this dataset, the algorithm resulted in a Root Mean Squared Error (RMSE) of 5.2 BPM.

I) Training the Filter: As described above, the Savitzky-Golay filter's number of points parameter (n) is recalculated for each new window of data, based upon the previous window's estimated respiratory rate. This raises the question, if the i^{th} window's filter is based upon the $(i-1)^{th}$ window, how is the filter for the first window set? We answered this question by setting the initial respiratory rate to a value (r_{init}) and then training the filter with n_{tr} incomplete windows of training data. During these training windows, no respiratory rate is output, but a respiratory rate is calculated and is used to set the number of points parameter for the next window's filter. Thus, in our implementation, there are no estimations the first $\Delta_w * n_{tr} = 0.5 * 10 = 5$ seconds. This process leads to the convergence of estimated respiration rate to the correct rate by the end of the 5 second training period.

Further testing revealed that, to a very large degree, the choice of r_{init} was overwhelmed by inclusion of n_{tr} training windows. This matches well with the findings presented in section III-B regarding the convergence limits of the algorithm when faced with instantaneous jumps in respiratory rate of varying sizes.

C. Extrema Detection

Once the RSSI signal is filtered, extrema are detected in the filtered signal, and the respiratory rate is calculated.

Note that, if a window contains z extrema, the window contains (z-1)/2 breaths, because each breath contains a maximum (peak) and a minimum (valley) and the first breath is marked by three extrema (e.g. peak, valley, peak). For example, if there are 5 extrema (3 peaks and 2 valleys or the other way around) there would be (5-1)/2=2 breaths detected. Note also that, in this case, the 2 breaths should not necessarily be thought of as occupying the entire window, but they might be appropriately thought of as occupying either the entire window or the sub-window that extends from the first extremum to the last extremum. This observation raises a question: 'which is the true respiratory rate: the number of breaths in the window divided by the number of seconds in the window, or the number of breaths divided by the time covered by those breaths?'

We answered that question by considering two cases. In case one, the more common case, the initial or final extrema is separated from the window boundary by a small margin. Here, the time between the initial and final extrema and the window boundaries represents a partial breath which was cut off by the window boundary before an extrema could be reached, and we divide the number of breaths by the amount of time between the extrema in order to get the number of breaths per second in the time window. In case two, the first or last extrema is separated from the window boundary by a large margin. In this case, excluding the time between the initial or final extrema and the window boundary from the denominator would create an artificially high respiratory rate. Thus, we divide the number of breaths by the size of the window.

Once we have divided by the appropriate length of time, we multiply by 60 sec/min to get the BPM in the time window. This value is the average respiratory rate of the entire window, and is recorded as the instantaneous respiratory rate associated with the moment that comes at the end of the window.

IV. TESTING METHODOLOGY

We investigated algorithm performance using the Bellyband and using a wired respiratory monitor. Data were gathered under a protocol approved by our university's Institutional Review Board (IRB)¹. The Bellyband was attached to each subject, along with a second, wired respiration measuring device: a Vernier Go Direct Respiration Belt [33], as shown in Figure 7. The Go Direct Respiration Belt was used to establish

¹The study protocol was approved by the Drexel University IRB under protocol number 1604004440.

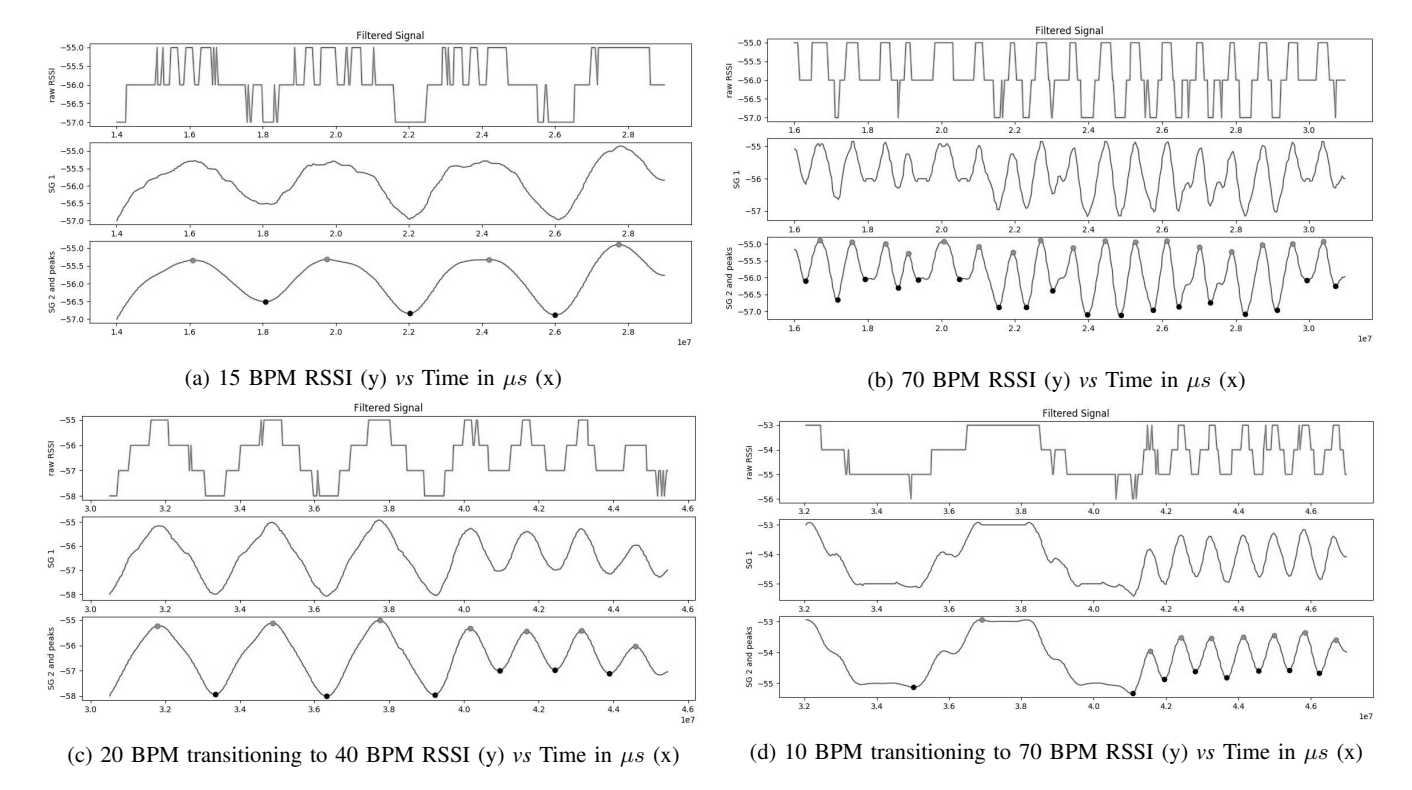


Fig. 6: Four sets of data filtered by the adaptive Savitzky-Golay Filter. In each image, the top line shows the raw RSSI data. The middle line is the same data after the first Savitzky-Golay filter. The bottom line shows the same data after the second Savitzky-Golay filter. The black and grey dots show the extrema detected by the algorithm. Note that the filter eliminates the noise while preserving the signal in all four sets of data. Note also that the filter performs well when the signal has a low dynamic range, as in Figure 6b, the respiratory rate changes moderately, as in Figure 6c, and the respiratory rate changes dramatically, as in Figure 6d.

ground truth respiratory rate. Both sensors recorded all data sets.

A metronome was set to click at a specific frequency which was a multiple of the desired respiratory rate (for example 60 clicks per minute when a respiratory rate of 15 BPM was desired). The test subject was instructed to time their breathing with the metronome, and a researcher observed them to make sure they were breathing at the specified rate.

Note that it is relatively easy to synchronize a breathing rate with a metronome rate as long as Equation 5 holds

$$\frac{\text{metronome rate}}{\text{breathing rate} \times 2} \in \mathbb{Z}^+$$
 (5)

This is because the inhale and exhale each take place over an integer number of clicks, and the subject can time their inhale and exhale length to a integer number of clicks without much training or expertise. At the beginning and end of each data set, the subject inhaled quickly and deeply, held their breath for 5 seconds, exhaled quickly and deeply, and held for 5 seconds. The signature of these opening and closing breaths allowed the signals from the Bellyband and the Go Direct Respiration Belt to be synchronized.

We gathered data during 25 trials. Each trial lasted 1 to 2 minutes. We gathered data in using seven different respiratory patterns, with experimental parameters summarized in Table II, and using the following ground-truth respiratory patterns for validation:

- i 15 BPM
- ii 15 BPM followed by 30 BPM
- iii 20 BPM followed by 40 BPM
- iv 20 BPM followed by 10 BPM
- v 30 BPM, then 15 BPM, then 30 BPM, then 15 BPM
- vi 70 BPM
- vii 10 BPM, then 70 BPM, then 10 BPM, then 70 BPM

We chose this mix of datasets because it included both low and high rates, constant rates, rates that changed multiple times, and instantaneous rate changes of varying intensity, and yet all of its rates could be synchronized with a metronome, giving us streams of data for which we could determine the underlying respiratory rate accurately and precisely.

Once the data was collected, we tested our algorithm. on window sizes of 2, 4, 6, 8, 10 and 15 seconds. Our data included sharp discontinuities in the respiratory rate (for example, datasets might change from 15 BPM to 30



Fig. 7: Bellyband and Vernier Go Direct Respiration Belt on subject. The Respiration Belt (below), a wired sensor, was used to verify ground truth respiratory rate. The datastreams from the sensors were synchronized by the subject taking a particularly deep breath at the beginning and ending of the data collection - creating a noticeable wave signature in both streams.

TABLE II: The experimental parameters used in our algorithm.

Symbol	Value	Definition		
W	15	size of data window in seconds		
Δ_w	0.5	window slide in seconds		
n_{tr}	10	number of training windows		
k	3	degree of the SG filter polynomial		
r_{init}	40	initial respiratory rate estimate		
r_{ll}	6	lower limit of likely respiratory rate		
r_{reset}	100	value to which respiratory rate esti-		
		mate was reset when r_{ll} was breached		
m	2	number of applications of the		
		Savitzky-Golay filter		
Δ_y	$0.1 \times \text{range}(\text{RSSI})$	threshold below which detected ex-		
		trema are discarded		

BPM instantaneously). During time windows which included h seconds of a higher respiratory rate (r_{max}) and l seconds of a lower respiratory rate (r_{min}) , the ideal algorithm would estimate the respiratory rate (r) to be a linear combination of the two rates (Equation 6):

$$r = \frac{(h \times \text{higher rate}) + (l \times \text{lower rate})}{h + l}$$
 (6)

Thus, we built this equation into the ground truth files against which we tested the algorithm. We calculated the RMSE, the bias, and the LOA of the algorithm over the entire dataset. Table III compares the RMSE of Extrema Peak Detection to the performance of the previous state-of-the-art Bellyband algorithm.

V. RESULTS AND DISCUSSION

Table II describes the values we used when implementing the algorithm described in Section III. RMSE is a common

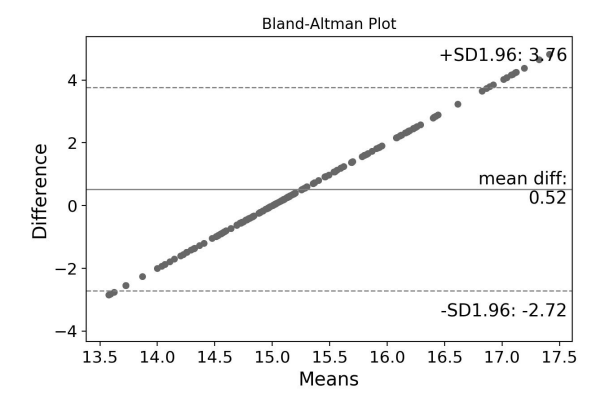
TABLE III: Average RMSE of two algorithms on 25 trials. Starting from the left: the 1st column shows the trials' respiratory rate(s), the 2nd column shows the number of trials which used that respiratory rate, the 3rd column shows the sum of the lengths of the trials with that respiratory rate (in minutes:seconds), the 4th column shows the previous state-of-the-art, which used a Gaussian Mixture Model (GMM) to fuse estimates from four different algorithms into a single estimate [15]. The 5th column (FED) shows Filtered Extrema Detection, the algorithm which is presented in this paper. The 6th column shows the average percent improvement of Filtered Extrema Detection over GMM on each set of trials with the same respiratory rate. Note that the averages in the final row are calculated as $(\sum_{i=1}^7 RMSE_i * TotalTime_i)/(\sum_{i=1}^7 TotalTime_i)$.

Rate(s) (BPM)	# trials	total time (m:s)	GMM (RMSE)	FED (RMSE)	RMSE Reduct.
15	5	9:00	4.0	1.2	70%
15, then 30	3	3:06	9.7	1.4	86%
10, then 20	4	4:00	7.3	4.3	41%
20, then 40	5	5:00	10.8	12.8	-18%
30, 15, 30, 15	4	5:20	8.4	2.4	71%
70	3	3:00	49.6	3.3	93%
10, 70, 10, 70	1	2:00	32.8	5.2	84%
Totals	25	31:26	13.0*	4.1*	68%*

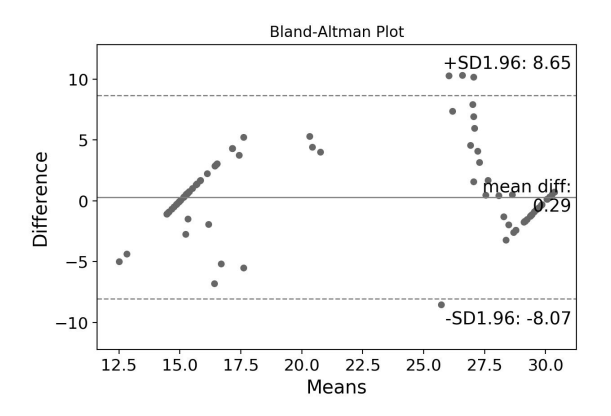
measure of how much a set of values deviates from verified values. We used RMSE to evaluate algorithm performance on each trial in the following way: when the algorithm processed a trial, it generated a respiratory rate estimate every 0.5 seconds. Upon finishing, it had created a list of time-stamped estimates. The RMSE is computed from these estimates against ground truth.

Table III charts the RMSE of two Bellyband algorithms. The first 7 rows list the RMSE of an algorithm on one type of trial (type is determined by the underlying respiratory rate of the subject during that trial). The final row contains averages and totals for the entire set of 25 trials. The 4th column (GMM) shows the performance of the previous state-of-the-art algorithm for detecting respiratory rate from a smart fabric with passive RFID on the data. GMM is a Gaussian Mixture Model algorithm, which fuses four different algorithms' estimates together [15]. The 5th column (FED) shows the results of the algorithm presented in Section III

As Table III shows, Filtered Extrema Detection's error rate is lower than the previous Bellyband algorithm's error rate by 68%, averaged across all trials. It also has a slightly lower error rate than the state of the art algorithms for detecting respiratory rate from ECG or IP. In a 2016 study, 314 algorithms designed to deliver respiratory rate from ECG, PPG, or IP data were tested. The best algorithm had a bias of 0 and a 95% LOA (the range falling within 1.96 standard deviations of the mean) of -4.7 to 4.7 [4]. On these 25 trials, Filtered Extrema Detection's bias was: 2.1 and its 95% LOA was (1.5, 2.7), comparable to the LOA of the best algorithm available for ECG, PPG, and IP. The 95% LOA ranges for two sample trials were (-2.72,



(a) Bland-Altman plot for a trial run in which a human subject breathed at a rate of 15 BPM for two minutes.



(b) Bland-Altman plot for a trial run in which a human subject breathed at a rate of 15 BPM for \approx 30 seconds, then at a rate of 30 BPM for 30 seconds.

Fig. 8: Example Bland-Altman plots from the human trial data collected, indicating the differences from the mean respiratory rate in BPM. 95% LOA ranges are given as the ± 1.96 Standard Deviation (SD) dashed lines in the plots.

3.76) at a 15 BPM respiratory trial, and (-8.07, 8.65) at a 70 BPM respiratory trial is given in Figure 8.

The algorithm took an average of 0.26 seconds to process one second of data, which cuts the previous algorithm's speed performance of 0.79 seconds by 67%.

VI. CONCLUSIONS AND FUTURE WORK

In this paper, we have presented a novel algorithm for measuring respiratory rate from the noisy, quantized signal produced by the Bellyband: a knit, smart fabric, wireless, passive, RFID sensor. The algorithm operates on the RSSI of the signal returned from the Bellyband. It filters the signal twice with an adaptive Savitzky-Golay filter, then detects extrema on the resulting wave. The algorithm was tested on data gathered in 25 trials, whose underlying respiratory

rate ranged from 10 to 70 BPM. Over the 25 trials, the algorithm averaged a 4.1 BPM RMSE. This result represents a 68% improvement over the previous state-of-the-art, and, though based on a less diverse and smaller dataset, suggests that the Bellyband sensor and the Filtered Extrema Detection algorithm might be made as or more accurate than sensors and algorithms currently in widespread use for respiratory rate detection, such as ECG and IP.

While the algorithm and testing regime presented here represent significant milestones for this project, additional progress remains to be made. The dataset included only deep breathing at constant respiratory rates by two adult test subjects in a controlled lab environment. These features of the dataset likely resulted in a higher signal-to-noise ratio than would result from normal or shallow breathing, a smaller/younger subject, or a non-lab environment. In the near future, we plan to gather a more diverse and larger dataset which will overcome these limitations. We will soon gather data from a diverse set of subjects which will be instructed to breathe normally (not intentionally deeply or intentionally steadily). We also anticipate a clinical trial on infants at a local hospital in the near future. At the physical layer, we intend to utilize interrogator radios on smartphone and/or portable devices, and denoise ambulatory sensing using a reference tag embedded into the garment with an interrogator worn about an ambulatory subject.

ACKNOWLEDGMENT

Our research results are based upon work supported by the National Science Foundation Division of Computer and Network Systems under award number CNS-1816387. Any opinions, findings, and conclusions or recommendations expressed in this material are those of the author(s) and do not necessarily reflect the views of the National Science Foundation. Research reported in this publication was supported by the National Institutes of Health under award number R01 EB029364-01 and award number U01EB023035. The content is solely the responsibility of the authors and does not necessarily represent the official views of the National Institutes of Health. This research was funded by the Commonwealth of Pennsylvania through the Commonwealth Universal Research Enhancement (CURE) program.

REFERENCES

- F. Q. AL-Khalidi, R. Saatchi, D. Burke, H. Elphick, and S. Tan, "Respiration Rate Monitoring Methods: A Review," *Pediatric pulmonology*, vol. 46, no. 6, pp. 523–529, 2011.
- [2] H. Chen, M. Xue, Z. Mei, S. Bambang Oetomo, and W. Chen, "A Review of Wearable Sensor Systems for Monitoring Body Movements of Neonates," *Sensors*, vol. 16, no. 12, 2016. [Online]. Available: http://www.mdpi.com/1424-8220/16/12/2134
- [3] Z. Zhu, T. Liu, G. Li, T. Li, and Y. Inoue, "Wearable Sensor Systems for Infants," Sensors, vol. 15, pp. 3721–3749, 02 2015.
- [4] P. H. Charlton, T. Bonnici, L. Tarassenko, D. A. Clifton, R. Beale, and P. J. Watkinson, "An Assessment of Algorithms to Estimate Respiratory Rate from the Electrocardiogram and Photoplethysmogram," *Physiological Measurement*, vol. 37, no. 4, p. 610, 2016. [Online]. Available: http://stacks.iop.org/0967-3334/37/i=4/a=610
- [5] Laerdal, "Laerdal Simbaby and Linkbox Product Page," http://www.laerdal.com/ us/item/245-02001, accessed: 2018-06-29.

- [6] D. Patron, T. Kurzweg, A. Fontecchio, G. Dion, and K. R. Dandekar, "Wireless Strain Sensor through a Flexible Tag Antenna Employing Inductively-Coupled RFID Microchip," in Wireless and Microwave Technology Conference (WAMICON), 2014 IEEE 15th Annual. IEEE, 2014, pp. 1–3.
- [7] D. Patron, W. Mongan, T. P. Kurzweg, A. Fontecchio, G. Dion, E. K. Anday, and K. R. Dandekar, "On the Use of Knitted Antennas and Inductively Coupled RFID Tags for Wearable Applications," *IEEE Transactions on Biomedical Circuits and Systems*, 2016.
- [8] W. Mongan, E. Anday, G. Dion, A. Fontecchio, K. Joyce, T. Kurzweg, Y. Liu, O. Montgomery, I. Rasheed, C. Sahin, S. Vora, and K. Dandekar, "A Multi-Disciplinary Framework for Continuous Biomedical Monitoring Using Low-Power Passive RFID-Based Wireless Wearable Sensors," in Proc. of IEEE International Conference on Smart Computing (SMARTCOMP), May 2016.
- [9] W. M. Mongan, I. Rasheed, K. Ved, S. Vora, K. Dandekar, G. Dion, T. Kurzweg, and A. Fontecchio, "On the Use of Radio Frequency Identification for Continuous Biomedical Monitoring," in *Proceedings of the Second International Conference on Internet-of-Things Design and Implementation*, ser. IoTDI '17. New York, NY, USA: ACM, 2017, pp. 197–202. [Online]. Available: http://doi.acm.org/10.1145/3054977.3055002
- [10] Y. Liu, A. Levitt, C. Kara, C. Sahin, G. Dion, and K. R. Dandekar, "An Improved Design of Wearable Strain Sensor Based on Knitted RFID Technology," in 2016 IEEE Conference on Antenna Measurements Applications (CAMA), Oct 2016, pp. 1–4.
- [11] MAGICSTRAP Technical Data Sheet, Murata, 11 2012.
- [12] Impinj Monza X-2K Dura Datasheet, Impinj, 3 2014, rev. 1.51.
- [13] Impinj, "Impinj Speedway Revolution," http://www.impinj.com/products/readers/speedway-revolution/.
- [14] Circular Polarity RFID Panel Antenna, RFMAX.
- [15] W. Mongan, R. Ross, I. Rasheed, Y. Liu, K. Ved, E. Anday, K. Dandekar, G. Dion, T. Kurzweg, and A. Fontecchio, "Data Fusion of Single-tag RFID Measurements for Respiratory Rate Monitoring," in 2017 IEEE Signal Processing in Medicine and Biology Symposium (SPMB), Dec 2017, pp. 1–6.
- [16] Impinj, "Application Note Low Level User Data Support," https://support.impinj.com/hc/en-us/article_attachments/200774268/SR_AN_IPJ_Speedway_Rev_Low_Level_Data_Support_20130911.pdf.
- [17] F. Adib, H. Mao, Z. Kabelac, D. Katabi, and R. C. Miller, "Smart Homes that Monitor Breathing and Heart Rate," in *Proceedings of the* 33rd Annual ACM Conference on Human Factors in Computing Systems. ACM, 2015, pp. 837–846.
- [18] C. Chen, Y. Han, Y. Chen, H.-Q. Lai, F. Zhang, B. Wang, and K. R. Liu, "TR-BREATH: Time-Reversal Breathing Rate Estimation and Detection," *IEEE Transactions on Biomedical Engineering*, 2017.
- [26] M. Browne, N. Mayer, and T. R. Cutmore, "A Multiscale Polynomial Filter for Adaptive Smoothing," *Digital Signal Processing*, vol. 17, no. 1, pp. 69–75, 2007.

- [19] O. J. Kaltiokallio, H. Yigitler, R. Jäntti, and N. Patwari, "Non-invasive Respiration Rate Monitoring using a Single COTS TX-RX Pair," in *Proceedings of the 13th International Symposium on Information Processing in Sensor Networks*. IEEE Press, 2014, pp. 59–70.
- [20] S. Šprager and D. Zazula, "Heartbeat and Respiration Detection from Optical Interferometric Signals by using a Multimethod Approach," *IEEE Transactions on Biomedical Engineering*, vol. 59, no. 10, pp. 2922–2929, 2012.
- [21] P. Marchionni, L. Scalise, I. Ercoli, and E. Tomasini, "An Optical Measurement Method for the Simultaneous Assessment of Respiration and Heart Rates in Preterm Infants," *Review of Scientific Instruments*, vol. 84, no. 12, p. 121705, 2013.
- [22] J.-H. Kim, R. Roberge, J. Powell, A. Shafer, and W. J. Williams, "Measurement Accuracy of Heart Rate and Respiratory Rate during Graded Exercise and Sustained Exercise in the Heat using the Zephyr BioHarness," *International Journal of Sports Medicine*, vol. 34, no. 06, pp. 497–501, 2013.
- [23] T. Flenady, T. Dwyer, and J. Applegarth, "Accurate Respiratory Rates Count: So Should You!" Australasian Emergency Nursing Journal, vol. 20, no. 1, pp. 45–47, 2017.
- [24] A. Savitzky and M. J. Golay, "Smoothing and Differentiation of Data by Simplified Least Squares Procedures," *Analytical Chemistry*, vol. 36, no. 8, pp. 1627–1639, 1964.
- [25] R. W. Schafer, "What Is a Savitzky-Golay Filter?" IEEE Signal Processing Magazine, vol. 28, no. 4, pp. 111–117, July 2011.
- [27] D. Acharya, A. Rani, S. Agarwal, and V. Singh, "Application of Adaptive Savitzky-Golay Filter for EEG Signal Processing," *Perspectives in Science*, vol. 8, pp. 677–679, 2016.
- [28] R. W. Schafer, "On the Frequency-Domain Properties of Savitzky-Golay Filters," 2011 Digital Signal Processing and Signal Processing Education Meeting, DSP/SPE 2011 Proceedings, pp. 54–59, 2011.
- [29] S. W. Smith, The Scientist and Engineer's Guide to Digital Signal Processing. San Diego, CA, USA: California Technical Publishing, 1997
- [30] J. Dombi and A. Dineva, "Adaptive Multi-round Smoothing Based on the Savitzky-Golay Filter," in *International Workshop Soft Computing Applications*. Springer, 2016, pp. 446–454.
- [31] W. Mongan, "Predictive Analytics on Real-Time Biofeedback for Actionable Classification of Activity State," PhD dissertation, Drexel University, 2018.
- [32] W. M. Mongan, I. Rasheed, K. Ved, A. Levitt, E. Anday, K. Dandekar, G. Dion, T. Kurzweg, and A. Fontecchio, "Real-time Detection of Apnea via Signal Processing of Time-series Properties of RFID-based Smart Garments," in Signal Processing in Medicine and Biology Symposium (SPMB), 2016 IEEE. IEEE, 2016, pp. 1–6.
- [33] Vernier, "Go Direct Respiration Belt," https://www.vernier.com/product/go-direct-respiration-belt/#tabspecifications, accessed: 2020-05-17.